Encapsulation of oil droplets using film-forming Janus nanoparticles

Geosmin Turpin,[1,2] Duc Nguyen,[1,2] Kathryn Isobel Sypkes,[1] Christopher Vega-Sánchez,[1,2,3] Tim Davey,[4] Brian S. Hawkett,[1,2] Chiara Neto[1,2,*]

1. School of Chemistry, Key Centre for Polymers and Colloids, The University of Sydney, NSW 2006 Australia
2. University of Sydney Nano Institute, The University of Sydney, NSW 2006 Australia
3. School of Electromechanical Engineering, Costa Rica Institute of Technology, Cartago 159-7050, Costa Rica
4. Dulux Australia, Innovation Centre, 1956 Dandenong Road, Clayton, VIC 3168, Australia
*corresponding author: chiara.neto@sydney.edu.au

Abstract

Polymer Janus nanoparticles with one hard crosslinked polystyrene lobe and one soft film-forming poly(methyl methacrylate-*co*-butyl acrylate) lobe were synthesised by reversible addition–fragmentation chain transfer (RAFT)-mediated emulsion polymerisation. The Janus nanoparticles adsorbed to oil/water and air/water interfaces, where the soft lobes coalesced, forming films of thickness between 25 nm-250 nm; droplets of silicone oil and dodecane could be stably encapsulated in polymer in this way. When prepared by mechanical mixing without additives, capsules of diameter 5-500 μm could be prepared, and with additives and application of heat, capsules of diameter around 5 μm were achieved, even with highly viscous silicone oil (20,000 cSt); in a microfluidic device, monodisperse capsules of diameter 180 μm could be formed. The particles were weakly surface active and spontaneously assembled themselves at air/water interfaces. When added into a paint formula the oil capsules improved the stain resistance of paint films. Silicone oil leakage from the capsules could be mitigated by incubating the capsules with silica nanoparticles, on which silicone oil reacts creating grafted layers.

ORCID

Turpin https://orcid.org/0000-0002-9323-7925
Nguyen https://orcid.org/0000-0001-8226-0129
Davey https://orcid.org/0000-0003-2316-3702
Vega-Sanchez https://orcid.org/0000-0002-2174-8291
Hawkett ttps://orcid.org/0000-0001-7609-0127
Neto https://orcid.org/0000-0001-6058-0885

Keywords: polymer shell, polymer nanoparticles, emulsion polymerization, self-assembly, thin polymer film

Introduction

The encapsulation of liquids is widely useful in many industries, with active areas of research ranging from improving drug delivery in medicines[1, 2] and active ingredients in personal care products[3] to improving vitamin content[4] and introducing functional ingredients into food.[5] Sustained or stimulus-responsive release of active ingredients from capsules can lead to self-healing properties.[6] Surface properties can be enhanced by capsules, with the sequestration of bioactive agents conferring antifouling properties to coatings[7] or the formation of self-cleaning systems.[8] Encapsulating a low surface energy system such as silicone oil can allow for improved hydrophobicity in paint,[9] while overcoming the dewetting or cratering that could arise if the silicone oil was simply mixed in.[10]

With such a wide variety of applications, it follows that there are many types of polymer microcapsules, synthesised through a diverse range of processes. These have been well reviewed,[6, 11] and include chemical methods such as interfacial polymerisation, *in situ* polymerisation and layer-by-layer assembly as well as physicochemical methods driven by self-assembly including sol-gel encapsulation, supercritical CO_2, spray-drying, co-extrusion, coacervation and solvent evaporation.

Crucial to applications is the fine control of the size and dispersity of capsules, which allows for more highly controlled dosage and release of active agents.[12 13] Much attention is given to the formation of microcapsules, on the scale of microns or smaller, as droplets larger than this can negatively impact bulk properties such as increasing viscosity,[14] or causing mechanically weaker polymer matrices.[15]

Many encapsulation methods use an intermediate Pickering emulsion templating step – in which particles stabilise the interfacial region - to allow for finer control of droplet dimensions and interfacially enriched material, translating to better control of capsule diameter and physicochemical properties of the eventuating capsule shell.[16] The formation of Pickering emulsions can also prove a challenge, as particles are kinetically rather than thermodynamically trapped to an interface, and the creation of droplets requires the addition of surfactants,[14] which can have drawbacks such as aggregation or extrusion from the surface,[17] adding water sensitivity[18] and affecting mechanical properties.[19]

Janus nanoparticles (JP) are a promising solution to this problem, being able to fulfil the role of Pickering stabiliser by jamming interfaces while being surface active,[20-23] creating thermodynamically stable systems.[24] JP can be inorganic,[25] combinations of organic and inorganic,[26] or fully polymeric.[27] Fully polymeric JP can be finely tuned through synthetic control, including lobe proportions, mechanical properties and amphiphilicity, influencing their interfacial adsorption and subsequent stabilisation behaviours.[24, 28-30]

Capsule stability and integrity are a concern for applications requiring a sustained release or a long shelf life, as pores or cracks in shells can cause uncontrolled release of active ingredients, or complete mechanical capsule failure resulting in premature release. Pickering emulsions

made from polystyrene/-poly(styrene-*co*-acrylic acid) (PS/P(Sty-*co*-AA)) JP used to encapsulate hexadecane droplets by mechanical vortexing demonstrated a 40% viability after 100 hours.[31] To improve this short shelf-life, the polymeric JP-stabilised Pickering emulsions need to be converted into a polymer capsule, often involving the use of physical or chemical crosslinking, such as by UV-light,[32] heat, and radical generation,[24] extreme salt concentrations, extreme pH levels or otherwise fine control of pH.[33 34] These extreme conditions favour shell formation, improving shelf stability, but may have the undesirable impact of lowering the activity of encapsulated ingredients.

This motivates the exploration of 'gentler' Pickering encapsulation methods suitable for thermally or chemically labile agents, such as enzymes, with some recent methods of interfacial crosslinking showing promise.[35] Other methods for achieving this require careful selection of particles; for example, alternating cationic and anionic latexes[36] or polysaccharide particles[37] cause electrostatic stabilisation of Pickering emulsions demonstrating a shelf-life of over a year. Some success has been demonstrated using poly(TPGDA)/poly(methacryl oxypropyl dimethylsiloxane) JP to stabilise emulsions made from their monomers for over 6 months,[38] however this requires a very specific set of JP and liquids to encapsulate.

What is still missing is a more generally applicable encapsulation technique that allows tunability, stability and longer shelf-life of the capsule, without requiring the use of harsh agents that diminish the activity of the encapsulated ingredients. Here, we demonstrate that snowman-shaped film-forming JP are a promising solution to this requirement. The snowman-shaped geometry of these JP has been previously shown in systems with high glass transition temperature (T_g) lobes,[39] and the synthesis mechanism is similar in the presence of low T_g, film-forming lobes (Scheme 1). The synthesis process involves the use of an amphiphilic macro-RAFT agent used as a stabilizer to produce crosslinked polystyrene seeds.[39] By swelling the cross-linked seed particles, snowman-shaped nanoparticles were synthesized with different chemical compositions.

We recently showed that these snowman JP made with a hard crosslinked polystyrene seed and a soft film-forming poly(methyl methacrylate-*co*-butyl acrylate) (P(MMA-*co*-BA)) lobe spontaneously adsorb to the interface of pigments and encapsulate them in a thin film of polymer, as the low T_g P(MMA-*co*-BA) lobes coalesce, without requiring chemical or thermal crosslinking.[40, 41] Our synthetic approach allowed the fabrication of large volumes of JP, sufficient for use in commodity paints. The encapsulation of pigment particles improved the stain resistance in paint coatings by reducing stain penetration on the hydrophilic inorganic pigment particles.

In this work, three different types of polymer JP were synthesised, and the most stable was used for encapsulation. For the first time newly synthesised film-forming snowman Janus nanoparticles were shown to adsorb and assemble into thin films on the surface of silicone oil droplets, leading to the encapsulation of the liquid droplets, without the need for high temperature heating or cross-linking agents, which makes them suited to encapsulating temperature- and chemical-labile active ingredients (Scheme 1b). The JP particles encapsulated

droplets of silicone oil of different viscosity (10 cSt and 20,000 cSt) and of dodecane, suggesting that the encapsulation would be effective for a wide range of oils and a wide range of viscosity. The produced oil capsules were integrated into a commercial paint formulation for the first time, improving stain resistance of the paint coating.

Materials and methods

Materials for JP synthesis

2-(Butylthiocarbonothioylthio)propanoic acid (BuPATTC), 2-([(dodecylsulfanyl)carbonothioyl]sulfanyl)propanoic acid (DoPAT) and dibenzyl trithiocarbonate (DBTTC) RAFT agents were provided by Dulux Australia and used as received. Butyl acrylate (BA), methyl methacrylate (MMA), acrylic acid (AA), styrene (Sty), methacrylic acid (MAA), divinyl benzene (DVB) hydroxy ethyl acrylate (HEA), sodium styrene sulfonate (StS), dioxane, propylene glycol, sodium dodecyl sulphate (SDS), ammonium persulphate (APS), 4,4′-azobis(4-cyanovaleric acid) V501, 2,2'-azobis(methylbutyronitrile) (Vazo 67), 2,2'-azobisisobutyronitrile (AIBN), ammonium hydroxide (25%) were purchased from Merk. Inhibitors in BA and MMA were removed by running the monomers through a column packed with inhibitor remover (Sigma). Inhibitors were removed from styrene using a column packed with basic alumina (Sigma). Other monomers were used as received.

Materials for capsule formation and characterisation

KCl, NaCl, $CaCl_2$, NaOH, HCl as well as analytical-grade acetone and ethanol were purchased from Sigma-Aldrich (Castle Hill, Australia) and used without further purification. Ammonium hydroxide (28% NH3 in water, w/w) was purchased from Ajax Finechem (Sydney, Australia). Ultrapure water was obtained from a Millipore Direct-Q 5 UV-R system (18.2 MΩ). Water-based, pigmented, white acrylic commercial paint was supplied by DuluxGroup

Methods:

JP Synthesis and characterisation

Synthesis of carboxylate and SDS stabilized JP

Film forming carboxylate and SDS stabilized JP were synthesized in the same manner as in our previous work and as follows.[41]

Synthesis of macro-RAFT diblock BuPATTC-(BA_5-*b*-AA_5) ([BA]/[AA]/[RAFT] ~5/5/1)

BuPATTC (7.7 g), AIBN (0.3 g), AA (11.6 g) in dioxane (40 g) was mixed in a 250 mL round bottom flask. The flask was sealed, magnetically stirred and sparged with nitrogen for 10 minutes. The reaction was carried out by heating at 70 ^oC for 3 hours under constant stirring. To the polymer solution, BA (20.7 g), AIBN (0.3 g) were added and mixed. The flask was sealed, deoxygenated with nitrogen for 10 minutes and then heated at 70 ^oC for another 3 hours under constant stirring. The final copolymer solution had 52 % solids.

Synthesis of seed latex using BuPATTC-(BA_5-*b*-AA_5)

In a 1L beaker, macro-RAFT solution (20.0 g) was dispersed in water (500.0 g) to yield a yellow dispersion. Ammonium hydroxide (25% solution in water) was added to the macro-RAFT solution to raise the pH to 9.3 producing a clear yellow solution. The solution was transferred to a 1 L round bottom flask containing V501 (0.3 g) which was subsequently sealed and purged with nitrogen for 10 minutes. The whole flask was then immersed in an oil bath with a temperature setting of 70 ^{o}C and was magnetically stirred. A deoxygenated styrene solution (50 mL, 45.3 g) was injected into the flask, while in the 70 ^{o}C oil bath, at a rate of 10 mL/hour. Upon completion of feeding, the heating was continued over 12 hours to produce yellow latex containing a small amount of polymer beads. The beads were subsequently removed by centrifugation, yielding semi-transparent yellow latex with 9.2% solids. Particle sizes of 5 nm were measured by dynamic light scattering (Zetasizer, Malvern Instruments).

Synthesis of 'Metastable JP'

Seed latex (251 g) was added to a 1L round bottom flask containing V501 (0.6 g) which was then followed by an addition of DVB (6.6 g). The flask was subsequently sealed and purged with nitrogen for 10 minutes. The whole flask was then immersed in an oil bath at 70 ^{o}C and was magnetically stirred. After 1 hour of heating, a deoxygenated MMA/BA solution (1:1 by weight) (50 mL, 45.9 g) was injected into the flask, while in the 70 ^{o}C oil bath, at a rate of 25 mL/hour. Upon completion of feeding, 7.5 g of 2% SDS solution was added. Another amount of deoxygenated MMA/BA solution (1:1 by weight) (70 mL, 64.2 g) was injected into the flask, while in the 70 ^{o}C oil bath, at a rate of 35 mL/hour. The heating was continued overnight to produce yellow latex. After filtering with 80 micron mesh, the final latex had 37% solids. Further details of synthesis and characterisation (GPC and NMR) of this system have been previously published.[41]

Synthesis of macro-RAFT DBTTC-poly(Styrene)-*block*-poly(BA-*co*-AA) ([Sty]/[BA]/[AA]/[[DBTTC] ~ 80/120/60/1)

DBTTC (0.6g), AIBN (0.08 g), AA (9.2 g), BA (32.6 g) were dissolved in dioxane (40.0 g). This solution was stirred magnetically and purged with nitrogen for 10 minutes. The reaction was then heated at 70 ^{o}C for 2.5 hours under constant stirring. Sty (17.7 g), AIBN (0.1 g) was then added to the polymer solution. The reaction vessel was sealed, deoxygenated with nitrogen for 15 minutes and then heated at 70 ^{o}C for another 12 hours under constant stirring. The final copolymer solution had 53% solids. Estimated macro-RAFT structure was DBTTC-Sty_{48}-*block*-(BA_{112}-co-AA_{56}).[40]

Crosslinked PS seed synthesis using DBTTC-poly(Sty)-*block*-poly(BA-*co*-AA)

The triblock copolymer (10.0 g) was dispersed in water (500.0 g) containing ammonium hydroxide (1.6 g, 25% in water) to yield a yellow solution with pH 9. Sty (25g), DVB (2.5 g, 80%) was added to the macro-RAFT solution and thoroughly dispersed by a mechanical stirrer to obtain yellow emulsion. This was poured into a 1 L round bottom flask containing V501 (0.15 g) which was subsequently sealed and purged with nitrogen for 15 minutes. The reaction was carried out in an oil bath with a temperature setting of 70 ^{o}C and was

magnetically stirred. The reaction was carried out in 12 hours to produce yellow latex with 6.2% solids and average particle size of 56 nm by DLS.

Synthesis of 'Large JP 'using triblock DBTTC-poly(Sty)-*block*-poly(BA-*co*-AA) macro-RAFT agent

Crosslinked seed latex (301 g) and water (301 g) was added to a 1L round bottom flask containing V501 (0.6 g). The flask was subsequently sealed and purged with nitrogen for 10 minutes. The whole flask was then immersed in an oil bath with a temperature setting of 70 ^{o}C and was magnetically stirred. A deoxygenated MMA/BA solution (1:1 by weight) (45.9 g) was injected into the flask, while in the 70 ^{o}C oil bath, at a rate of 20 mL/hour. After 2.5 hours, another 64.3 g monomer solution of MMA/BA (1:1) was injected into the flask at a rate of 35 mL/hour. Upon completion of feeding, the heating was continued overnight to produce white latex. The final latex had 17.5% solids with an average particle size of 93 nm (Zetasizer, Malvern Instruments). Further details of synthesis and characterisation (GPC and NMR) of this system have been previously published.[40]

Synthesis of 'Stable JP' using DoPAT-poly(HEA-*co*-AA-*co*-StS)

Synthesis of macro-RAFT DoPAT-poly(HEA-*co*-AA-*co*-StS) ([HEA]/[AA]/[StS]/[RAFT] ~ 30/5/5/1)

A solution containing DoPAT (3.35 g), AA (3.45 g), StS (9.96 g), HEA (33.33 g), Vazo-67 (0.2 g), water (30 g) and propylene glycol (30 g) was prepared in a 250 mL round bottom flask. After nitrogen sparging for 10 minutes, the reaction was carried out in oil bath at 70 ^{o}C for 3 hours. The final clear solution had 43% solids (~95% conversion), Mn~7200 g/mole and Đ of 1.14 by aqueous GPC. Estimated macro-RAFT structure was DoPAT-(HEA_{29}-co-AA_5-co-StS_5).

Synthesis of seed latex

In a 2L round bottom flask, the Macro-RAFT copolymer (100 g) was mixed with water (1L) to produce a clear yellow solution. Ammonium hydroxide solution (25%) was used to adjust the pH to 8.4. Styrene (100 g) and V501 initiator (0.6 g) was added and emulsified in the flask by simple magnetic stirring. After 15 minutes nitrogen sparging, the reaction was heated in an oil bath over 3 hours with continuous stirring. After filtering, the final had 11% solids, pH 6.9, containing 8 nm particles as measured by DLS. As seed latex was synthesized from a very hydrophilic polymer and a hydrophobic polystyrene, the material was not soluble in any organic GPC eluents. Therefore, GPC data for the polymer seed latex is not available.

Synthesis of Stable JP

In a 2 L reactor containing 1.1 kg seed latex, ammonium hydroxide (25%) was used to adjust the pH to 7.2. Under stirring, V501 (0.6 g) and DVB (12.5 g) was added. The reactor was sealed, nitrogen sparged for 15 minutes, then heated at 75 ^{o}C for 1 hour to produce white crosslinked seed latex. After raising the temperature to 80 ^{o}C, MMA/BA/MAA (48/48/4) (92.2 g) mixture was fed to the reaction at the rate of 120 mL/hour under continuous stirring. After 1 hour, an initiator solution of SDS (0.6 g), APS (0.3 g) and water (10 g) was added to the reactor. Another portion (138.3 g) of the same monomer mixture was added at the rate of 180

mL/hour under continuous stirring. After monomer addition, the reaction was allowed to continue for another 2 hours. After filtering, ammonium hydroxide (25%) was used to adjust the latex pH from 5 to 8. The final product had 26% solids with an average particle size of 70 nm by DLS.

Properties of JP in aqueous dispersion:
A Zetasizer (Malvern Instruments) was used to both measure the zeta potential values and to estimate the hydrodynamic radii of Janus particles using Dynamic Light Scattering (DLS). All highly charged film forming JP had a background KCl salt concentration of 1.47 mM to ensure sufficient screening, with measurements being undertaken at 0.1 wt%. Both sets of measurements had a sample size of N=5, each comprising of 15 individual runs for DLS and 50 individual runs for Zeta potential. Salt concentration studies were carried out at pH 7.9. Measurements on Metastable JP were carried out at 0.17 wt% for salt concentration studies, and 4 wt% for pH studies.

Interfacial behaviour of JP: Interfacial tension measurements were performed using a goniometer (Dataphysics OCA 50) in a glass cuvette sealed with hydrophobic tape with a blunt needle (SNS-D 05/25) inserted through the middle. Measurements were run for 1200 s until a pseudo-equilibrium was reached. Measurements were performed in triplicate for each system.

Forming Janus films on solid substrates: A silicon wafer was dipped vertically into a suspension of 4 wt% JP at 6 mm/min (KSV NIMA dip coater) and the suspension allowed to dry in air. The horizontal dip coating was performed by manually lowering the surface to just touch the top of the JP suspension and the wet film was allowed to dry in air.

Mechanical encapsulation: Silicone oil of viscosity 10 cSt, 20,000 cSt and *n*-dodecane were used as model oils. The encapsulation of small silicone oil droplets (around 5 μm in diameter) was performed using the details in Table 1 and by using an overhead mixer at 1850 rpm for 10 minutes.

Table 1 Details of formulation used to perform encapsulation by mechanical mixing in the presence of additives.

Materials	**Weight (g)**
Stable Janus Particles (25 wt.% solids)	10
Silicone oil 20,000 cSt (80wt %)/Optifilm 300 (20 wt.%)	10
ASE60	1.5
NH_4OH (28 wt.%)	0.21 (9 drops)
Deionised Water	10

When the JP and the silicone oil/Optifilm blend were mixed, a single faintly yellow phase was achieved. ASE 60 was added into above emulsion at once and mixed for 30 seconds. The obtained mixture was very viscous. NH_4OH (28 wt.%) was added into above mixture and mixed for 30 seconds, followed by dropping deionised water at 1850 rpm over 10 minutes. The obtained emulsion was heated at 80°C oil bath for 5 minutes under slow mixing to form the encapsulation shells.

Microfluidic encapsulation:
Encapsulation of 180 µm silicone oil droplets using JP was achieved using a microfluidic droplet chip (Dolomite Droplet Junction Chip, 190µm etch depth, Part No. 3000436). Prior to use, the droplet chip was thoroughly cleaned by sonication in Milli-Q water (18.2 MΩ), ethanol and acetone (ACS grade) for 1 min to 3 min each, and blown dry with high purity nitrogen (>99.99%, BOC Ltd), followed by plasma cleaning (Harrick Plasma, model PDC-002, 30W) for 3 min to produce highly hydrophilic channel walls. The continuous phase was Milli-Q water with a range of JP particle concentrations (0.6wt% - 7.5%wt%) and pH conditions (3.5 – 8.5), while the disperse phase was 10 cSt silicone oil (Sigma Aldrich).

Both water and oil were pumped using a pressure controller (OB1, Elveflow) and the flow rate was monitored using two flow sensors, one for each phase (MFS3 or MFS4, Elveflow). Stable droplets were collected at water flow rates from 500 to 1000 ul/min at oil flow rates of 1 to 8.5 ul/min. Due to clogging of the microchannel upon use of flocculated JP, only well dispersed JP could be used, and this led to capsules that were delicate, so could only be collected using an upside-down vial.

Application of encapsulated silicone oil in a stain resistant coating
Encapsulated oil emulsion (2 g) was blended with 18 g of Dulux LS W&W by an overhead stirrer at 2000 rpm for 1 min to produce well mixed paint. This paint was then applied to industry-standard Leneta cards and left in the oven overnight. Coffee and blue food dye was applied to strips of paper covering dried paint samples via Pasteur pipette until soaking. Lines were drawn across the surface using grey lead pencil, a crayon, and finally by manually scuffing with a piece of rubber. All stains and marks were allowed to dry for an hour before dye-soaked paper strips were removed. Surfaces were then cleaned 4 times with cleaning spray and paper towel, after which the samples were dried in an oven at 50 °C overnight.

Results and Discussion

Synthesis and characterisation of JP
Janus particles were synthesized by polymerization-induced self-assembly (PISA)-RAFT emulsion polymerization, following the process established in our previous works.[40, 41] A detailed procedure is presented in Materials and Methods. Briefly, as shown in Scheme 1, polystyrene (PS) seed particles were formed by controlled living free radical emulsion polymerization of styrene monomer in a solution containing micelles of amphiphilic diblock macro-RAFT copolymers (described below) in the presence of V-501 initiator at 80 °C for 3-

12 hours. The macro-RAFT copolymers remain on the surface of the growing particle, keeping it stable in suspension. The seeds were cross-linked with DVB at 80 ºC for 1 hour. The second lobe of the Janus particles was formed by further feeding of MMA/BA (1/1, by weight) monomer solution, which created a lobe expelled by the crosslinked PS seeds in the presence of V501 or APS thermal initiators. This step produced snowman-shaped Janus nanoparticles, containing one hard crosslinked PS seed and one soft P(MMA-*co*-BA) lobe (T_g =4 °C).[41] As shown in the inset in Scheme 1a, as the P(MMA-co-BA) lobe is soft, it cannot easily be imaged by atomic force (AFM) or transmission electron microscopy (TEM). A similar synthetic approach has been shown recently to lead to all-PS snowman-shaped JP, in which the lobe shape can be clearly imaged by TEM, as shown in Scheme 1a.[40, 41]

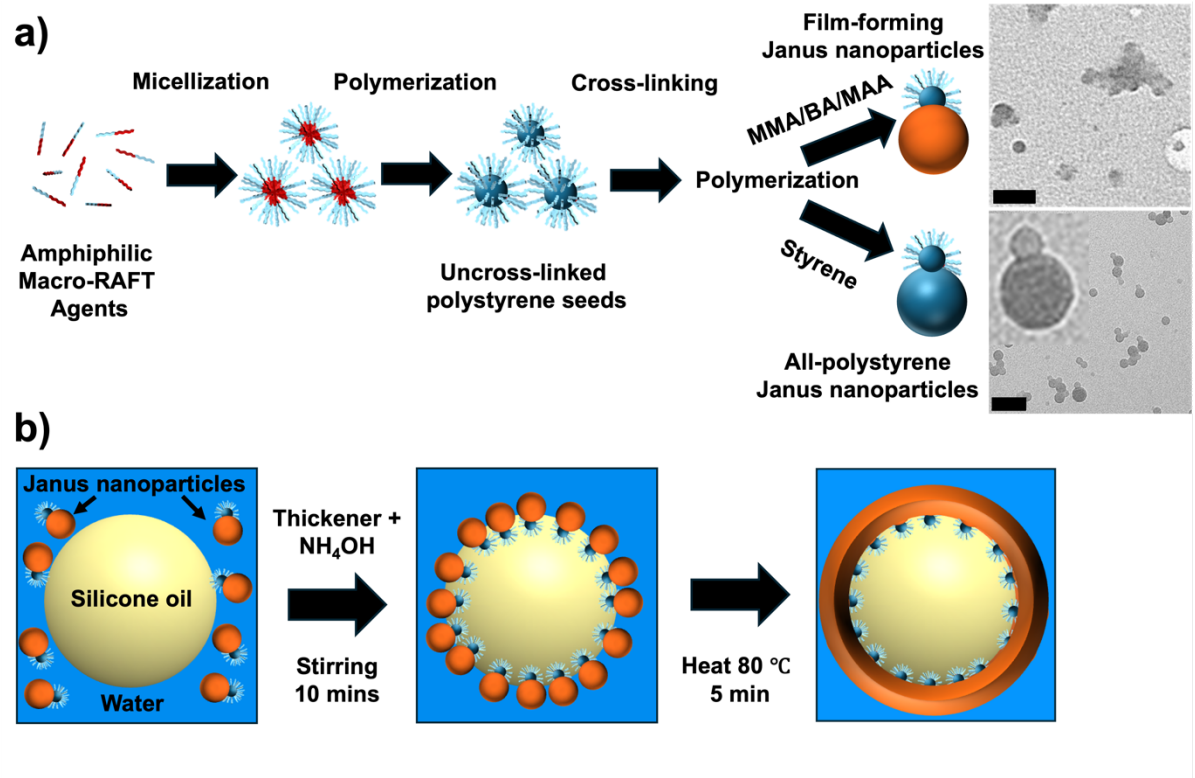

Scheme 1. Schematic of the synthesis process for polymer Janus nanoparticles and subsequent application to encapsulate silicone oil droplets. a) Seeded emulsion polymerization stabilized by amphiphilic macro-RAFT copolymers to form Janus nanoparticles. Macro-RAFT copolymers (red hydrophobic chains and blue hydrophilic chains) self-assemble into micelles, and styrene is continuously fed to form seed nanoparticles; after cross-linking of the seed, a second soft lobe is formed by polymerization of the (MMA/BA) or (MMA/BA/MAA) monomer solutions on the seed particle surface. The end product is a suspension of snowman shaped JP with a hard PS seed and a soft polymer lobe which is film-forming. Far right: TEM micrographs showing the film-forming nature of the second lobe in the JP with P(MMA/BA) lobe; all-polystyrene JP are included to demonstrate snowman geometry in the absence of spreading; a magnified image of 1 particle is included. Scalebars correspond to 100 nm. b) Proposed mechanism for encapsulating silicone oil droplets (10 cSt and 20,000 cSt) and dodecane droplets with film-forming JP. JP adsorb to the oil–water interface after shearing in the presence of thickener; heat, plasticizer and NH_4OH facilitates

soft lobe swelling and coalescence, resulting in a film-encapsulated oil droplet. For visual clarity, Janus particles are depicted at being adsorbed to perpendicular to the oil–water interface in a monolayer, however there is likely a distribution of orientations and capsule can be up to 10 particles thick.

In this study, three types of JP were prepared using three different macro-RAFT copolymers, which imposed charge on the surface of the particles and therefore affected their stability in suspension. In all cases the Janus particles were made of a polystyrene seed and a lobe of a softer polymer which was film-forming at room temperature. Their names and synthetic approach are described in the following:

i) '**Metastable JP'**: carboxylate and SDS stabilized JP using short chain diblock BuPATTC-(BA_5-*block*-AA_5) with 5 AA units. The produced JP were approx. 65 nm in diameter as found by dynamic light scattering (DLS), and at most pH carried on their surface negative charge from the deprotonated carboxylate groups originated from short block of P(AA_5) macro-RAFT and V501 initiator. SDS surfactant was added during the lobe formation step to further stabilize the JP. A TEM micrograph is shown in Fig. S5 showing film formation and coalescence between soft lobes. This type of JP was found to be metastable, forming aggregates after 2 years shelf storage, with the average hydrodynamic diameter increasing from 65 nm to 100 nm.

ii) '**Stable JP**': carboxylate/sulfonate/sulphate stabilized JP using DoPAT-(HEA_{29}-*co*-AA_5-*co*-StS_5) with 29 HEA, 5 AA and 5 StS units. The JP particles were approx. 65 nm in diameter. The DoPAT macro-RAFT copolymer had built-in hydrophobic dodecyl group like SDS. This made it as an effective emulsifier, reducing the need to add the second poly(BA) block as in the case of BuPATTC-(BA_5-*block*-AA_5). This JP system had their surface covered with a variety of non-charged and charged stabilizers: steric stabilizer blocks (29 HEA for seed surface), carboxylate (from macro-RAFT, V-501), sulphonate (from 5 StS units on macro-RAFT) and sulphate (from APS initiator). Furthermore, 4% MAA was used in fed monomer solution during the lobe formation process. After neutralization with ammonium hydroxide at pH 8, the lobes were covered by additional negative charge, making it potentially more stable over long storage period. A TEM micrograph is shown in Fig. S6.

iii) '**Large JP'**: carboxylate stabilized JP using triblock DBTTC-Sty_{48}-*block*-(BA_{112}-*co*-AA_{56}) with ~56 AA units. These JP were approx. 93 nm in diameter and contained on their surface carboxylate charge from the 56 AA units per macro-RAFT chains and V501. No SDS surfactant was used. These particles were used for their large size that made it easier to image by atomic force microscopy (AFM, see below). A TEM micrograph is shown in Fig. S7.

Properties of JP in aqueous dispersion

As particle-particle interactions affect encapsulation efficacy and film formation, the effects of pH and salinity on the stability of aqueous dispersions of JP were investigated. Figure 1 shows the characterisation of the Stable JP which are the focus of this work (data for the Metastable JP shown in Supp Info S1). The Stable JP were around 65 nm in diameter (Figure 1b) and could be stably dispersed in NaCl up to 750 mM, due to their negative zeta potential and steric effects

caused by SDS adsorbed to the surface of the JP. Aggregates of particles appeared to form in the presence of divalent cations above 5 mM $CaCl_2$ (Figure 1b). Although the effects of cation bridging are well-reported,[42, 43] other latexes have shown to be stable in the presence of divalent cations 30-100 mM,[44] indicating a notable sensitivity to divalent cations relative to similar systems.

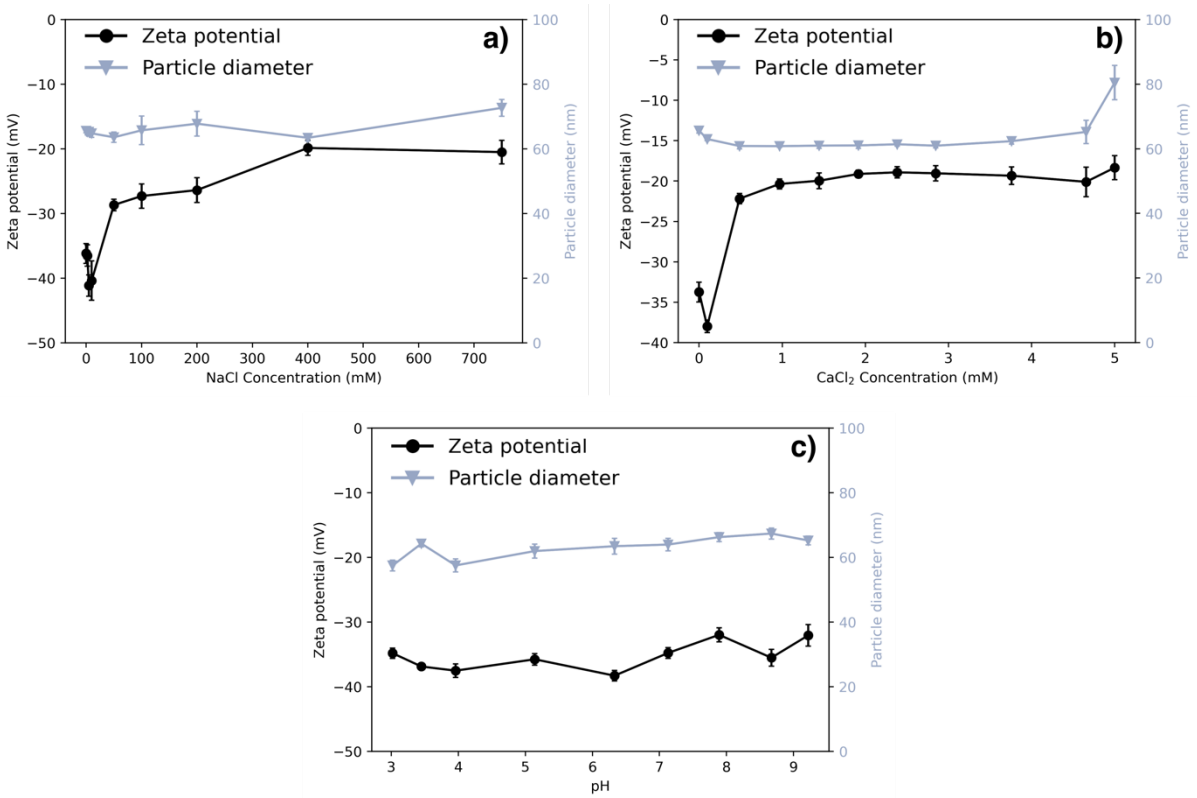

Figure 1. Zeta potential and particle diameter of Stable Janus nanoparticles (0.10 wt%) as a function of (a) NaCl concentration, (b) $CaCl_2$ concentration and (c) pH. The pH during salt concentration tests were 7.9. All systems had a background salt concentration of 1.5 mM KCl.

The Stable JP have a strongly negative zeta potential at all pH values tested, from pH 2.9 to 9 (Figure 1c), due to the carboxylate and sulfonate groups derived from the macro-RAFT agent and the SDS.[41] Protonation on sulphonate groups is known to be less sensitive to pH than for other groups, and the charge on SDS did not change with pH. In contrast, the Metastable JP were negatively charged but more sensitive to pH (Supp Info S1c), due to the deprotonation of the MMA lobe with a pKa of 4.5.[45]

Interfacial behaviour of JP

Stable JP were confirmed to be weakly surface active via pendant drop tensiometry, with oil–water interfacial tension decreasing with particle concentration for both silicone oil (Figure 2a) and dodecane (Figure 2b). A notable change in interfacial tension was observed at particle concentrations above 5 mg/mL. The dynamics of JP adsorption at the oil/water interface was relatively slow for both silicone oil and dodecane, taking over 10 minutes to reach plateau values at particle concentrations 20-60 mg/ml. This process occurs on timescales 1000 slower

than for molecular surfactants,[46] likely due to both the low driving force and the larger size, relative to individual molecules.

The impact of pH on JP surface activity was also explored (Figure 2c), with two local minima in silicone oil/water interfacial tension being observed (Figure 2d), one around pH 3.5 is likely due to the fact that at low pH, the magnitude of negative charge at the oil–water interface is decreased,[47] which led to a decreased charge-charge repulsion between the oil/water interface the particles; the second minimum in interfacial tension is around pH 9. This trend has also been reported previously by Jiang *et al.*,[22] with the gradual reduction in surface tension above pH 7 attributed to the weak Lewis acid characteristic of PMMA causing carbonyl groups to complex the Na^+ present in the base added to increase pH.[48] These phenomena contribute to the apparent adsorption rate differences between these systems; the low pH systems adsorb rapidly, lowering interfacial tension before measurement has commenced and resulting in an apparent lower interfacial tension at $t = 0$. In contrast, at high pH the JP have an initially higher interfacial tension as more time is required to overcome the electrostatic repulsion *via* the complexation mechanism.

Discussions of interfacial adsorption become more complex when film formation mechanisms are also hypothesized to contribute to encapsulation. These JP have been shown to form films over solid pigments as the soft lobes coalesce,[41] however latex particles adsorbed to fluid–fluid interfaces are shown to be more stable and less film-forming than their counterparts in 3D bulk dispersions due to unscreened dipole repulsion interactions through the oil phase.[49]

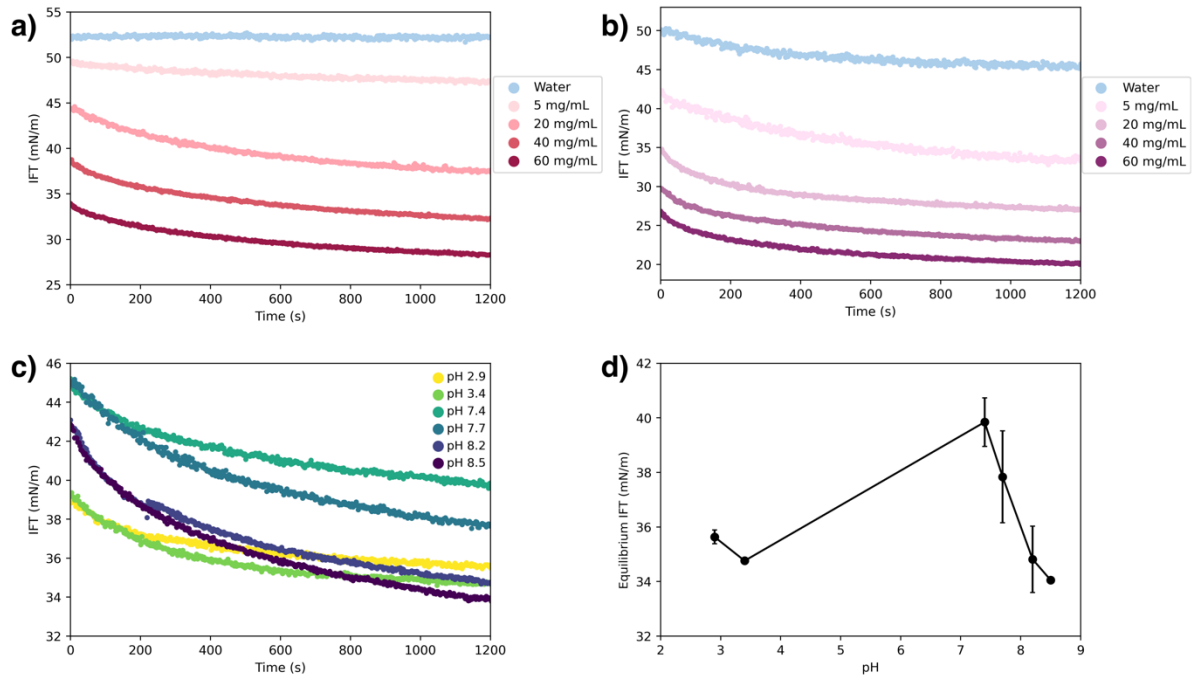

Figure 2. Surface activity of Stable JP at pH~8.35 over time at a) silicone oil/water and b) dodecane/water interfaces as a function of JP concentration. Curves presented are selected representations from triplicate measurements. c) Surface activity of 20 mg/mL JP at a silicone oil/water interface as a function of pH, showing interfacial adsorption over time. d) Equilibrium interfacial tension of a 20 mg/mL JP aqueous suspension at the silicone oil interface as a

function of pH, with vertical error bars representing standard deviation of triplicate measurements.

Film formation

Evidence of film formation at an interface was obtained by performing coating experiments onto flat solid substrates (Figure 3). These experiments were performed with the Large JP to facilitate imaging. Interfacial alignment of Janus particles can be random and depend on the shape of the interface,[50] but generally a stronger character of amphiphilicity and a high degree of charge asymmetry between the two lobes favour perpendicular alignment at water/oil interfaces.[51] [52] The PS seeds are more hydrophobic than the P(MMA-*co*-BA) lobe (films deposited vertically, with PS seeds exposed to the air, have a slightly higher water contact angle than those deposited horizontally, as shown in Table S1), so it was hypothesized that they would protrude into the air if JP were adsorbed to the air–water interface. This was tested by passing a solid substrate through the air/water interface vertically, akin to a Langmuir-Blodgett method, and by lowering a substrate horizontally to the air/water interface, more similar to a Langmuir-Schaeffer method.[53] The nanoscale topography of the resulting films was studied using AFM.

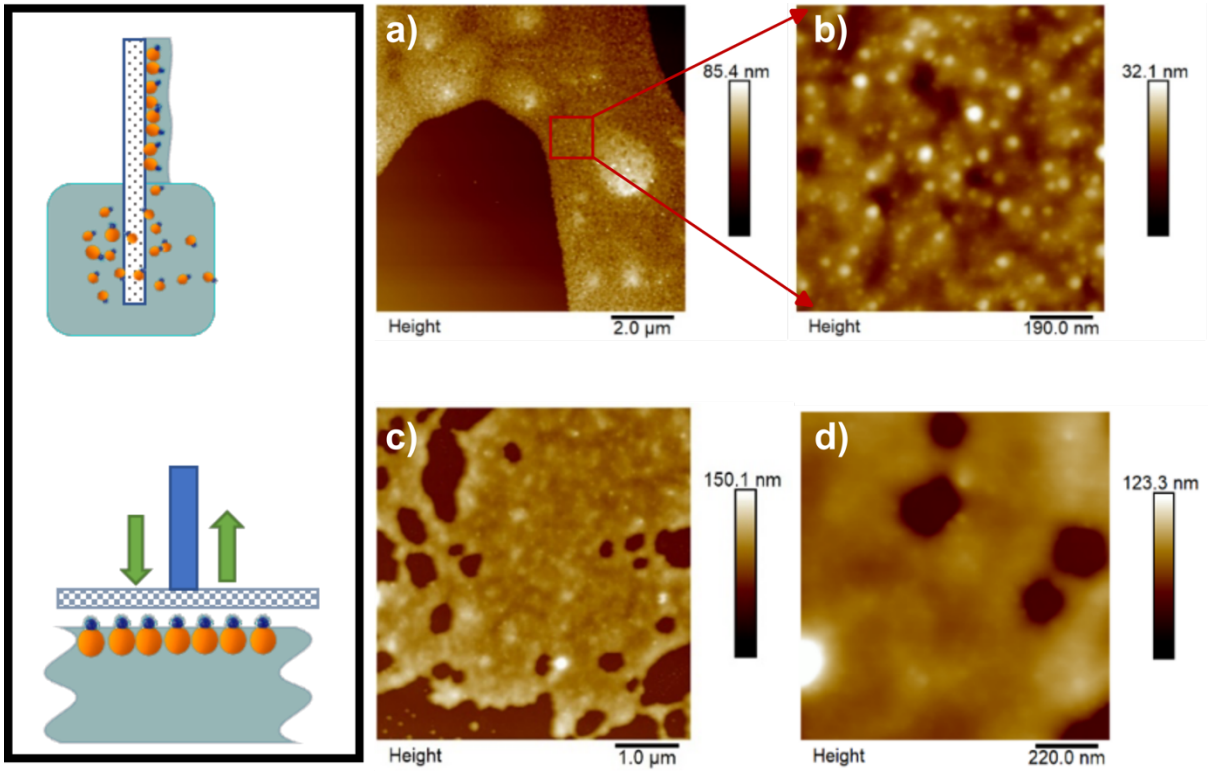

Figure 3. AFM micrographs of a-b) Janus film formed by dipping a silicon wafer vertically into a 4 wt.% JP suspension at the withdrawal speeds of 6 mm/min, and c-d) Janus films picked up by lowering horizontally a silicon wafer to the suspension surface. Inset left: schematics of hypothesized Janus orientation: top: deposition on a vertical substrate. The orange soft lobes orient towards the substrate and the blue PS heads face the opposite direction, as in Fig 3a-b. Bottom: a horizontal substrate picks up a Janus monolayer at the air/water interface as in Fig 3c-d, with the PS lobes facing the substrate.

A film was produced due the P(MMA-*co*-BA) lobes merging when the substrate was dipped in the vertical direction and the results are shown in Figure 3a) and b): bumps in the film are visible with size approximately matching the size expected for the hard PS seed particles. As shown in the schematic in the top inset of Figure 3, capillary forces drive particles to the substrate and together in the thin film of liquid suspension,[54] and as the water dries, the PS seed remain exposed to the air/water interfaces while the (MMA-*co*-BA) lobes merge.[55] The film thickness is consistent with the 20-25 nm films reported in our previous work encapsulating solids with these systems,[41] indicating a JP monolayer that underwent a film-formation process. A film was obtained also by horizontally lowering the substrate (Figure 3c-d)). The coalescence of film forming particles into latex films during drying is well established in the literature;[56, 57] the specific coalescence of the soft lobes on hard-soft snowman JP was previously established by the authors on solid particle surfaces.[41] This film formation is prominently visible in the TEM micrograph of 'Metastable JP' (Figure S5) while being subtly present as a corona around the darker polystyrene cores in for 'Stable JP' and 'Large JP' (inset in Scheme 1, Figures S6 and S7).

Having established that JP adsorbed to oil–water and air–water interfaces, forming films, the JP were used to encapsulate droplets of silicone oil.

Encapsulation of silicone oil using mechanical vortex

Stable JP suspensions were used to encapsulate silicone oil droplets, created by applying a mechanical vortex. As shown in Figure 4(a-b), silicone oil droplets of diameter in the range 50-500 μm could be achieved, following the addition of concentrated acid to JP suspensions. The fast addition of concentrated acids can lead to metastability and partial flocculation of the JP, which appears to be advantageous when encapsulating oil by mechanical stirring. Only silicone oil of low viscosity (10 cSt) could be stabilised in this way. JP capsules were successfully achieved at both pH 2.9 (Figure 4a), at which a local minimum of interfacial tension was observed and fastest adsorption kinetics hypothesized (Figure 2), and pH 7.4, at which maximum interfacial tension occurred.

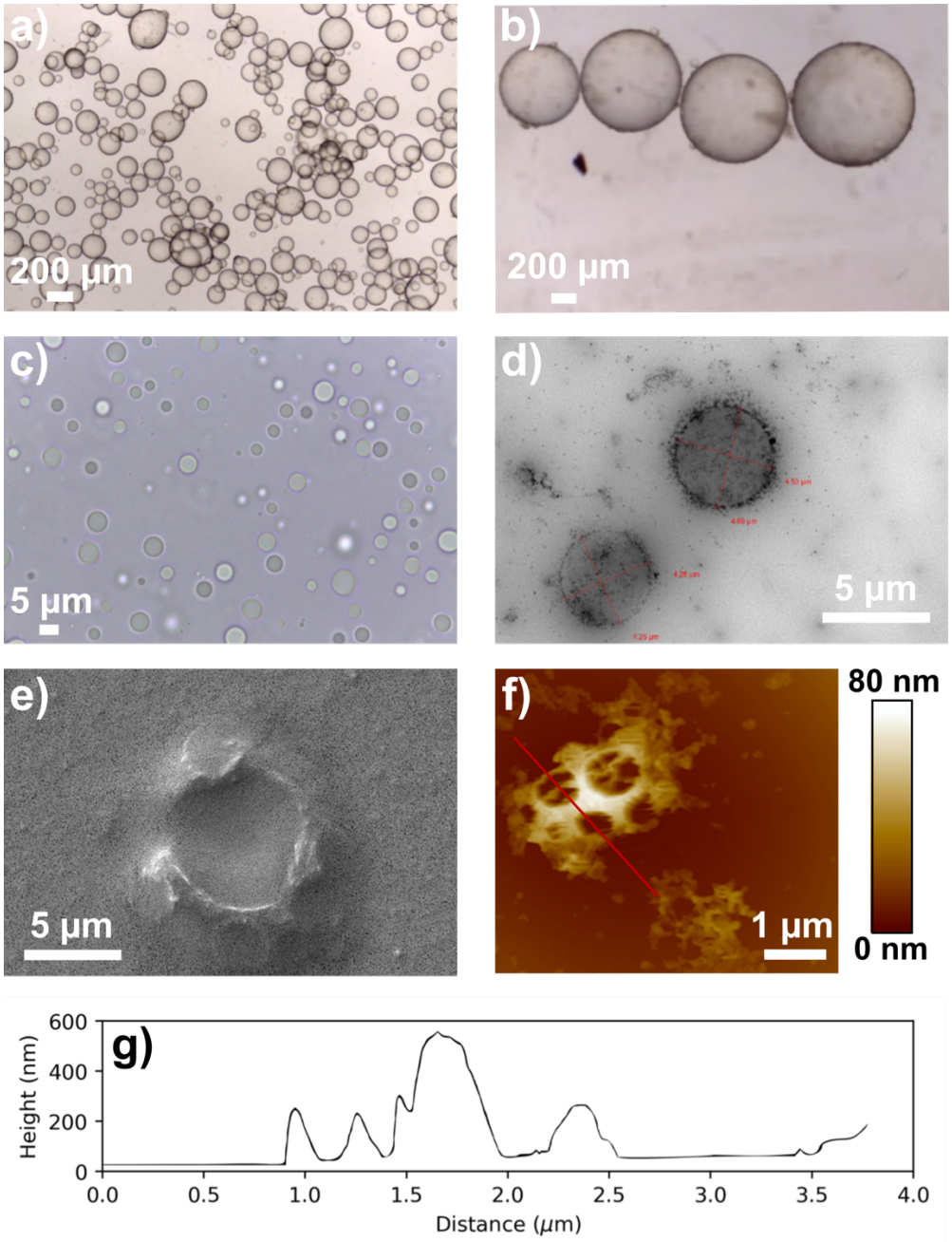

Figure 4. Silicone oil 10 cSt droplets encapsulated by Stable JP by mechanical vortexing. a-b) Optical micrographs of silicone oil droplets stabilised and encapsulated by 4 wt% Janus particles at pH 2.9 and pH 7.4, respectively. c) Silicone oil capsules of diameter 5 µm, stabilised by the addition of JP + additives Optifilm 300 and ASE60. d) TEM micrograph showing JP on the surface of silicone oil capsules. e) SEM micrograph showing dry structure of JP capsules around silicone oil droplet. f) AFM micrograph of the JP capsules dried on a silicon wafer after washing three times in Milli-Q water to remove the encapsulated silicone oil. g) Cross-sectional profile of the JP capsule along the red line in AFM micrograph in part f).

Mechanical encapsulation of silicone oil using additives and heat

To produce smaller oil droplets, additives were employed during the encapsulation. Smaller oil droplets of diameter 5 µm, as shown in Figure 4(c), could be encapsulated by addition of a plasticiser (Optifilm 300) which facilitated film formation, a thickener (ASE60) which

increased viscosity of the continuous medium to arrest coalescence, base (NH_4OH) and mild heating (see Materials and Methods).[58] Heating helped ammonium hydroxide to better penetrate and reach the carboxylic groups buried deep inside the polymer lobes. Once reacted, formed polyelectrolytes would take up water to swell. The heating might facilitate swelling, disintegrating the lobe in the process.

Capsules of lower diameter and polydispersity are desirable as they can be integrated into a matrix with lower detriment of its mechanical properties,[15] and with lower impact on matrix viscosity.[14] With these modifications, droplets of oil of higher viscosity, up to 20,000 cSt could be stabilised; oils of this high viscosity are harder to disperse and of higher interest as additives in paint. TEM (Figure 4d), SEM (Figure 4e) and AFM (Figure 4f) were used to confirm the presence of capsules around the oil droplets. Flocs of JP are visible on the surface of the capsules by TEM, and solid shells that collapse during drying are clearly visible by SEM and AFM. The capsules observed by AFM (Figure 4g) have a shell thickness between 50 nm and 250 nm, and appear not continuous but with circular holes, perhaps formed during drying. The AFM imaging of the dried capsules was conducted after washing away the encapsulated silicone oil. For comparison, a capsule imaged without further washing steps shows residues of the encapsulated silicone oil (Fig. S2).

Encapsulation of silicone oil using microfluidic methods

Control over polydispersity of the oil droplets was more easily achieved with microfluidics. Encapsulation of 10 cSt silicone oil droplets could be achieved using the Metastable JP suspensions without additional additives or flocculation using a microfluidic droplet chip with 190 µm etch depth. As shown in Figure 5, microfluidics allows fine control over diameter,[13] with monodisperse droplets of approx. 180 µm diameter being produced and collected. Janus particle concentration (0.6 wt% - 7.5 wt%), pH conditions (3.5 – 8.5) and flow rates (500 to 1000 µl/min water and 1 to 8.5 µl/min oil) were varied, with the longest capsule lifetime (6-14 days) being obtained at 2-4 wt% of JP and pH ~8. The different conditions tested are presented in Table S2. The produced capsules were comparable in stability to JP-stabilised hexadecane emulsion which showed 40% viability after 100 hours.[31] The prepared capsules were delicate, rendering them inappropriate for integration into coating formulations in their current iteration as they were only able to be collected using an upside-down vial (Figure S3). These findings provide a benchmark for future work with stronger capsules produced by microfluidics.

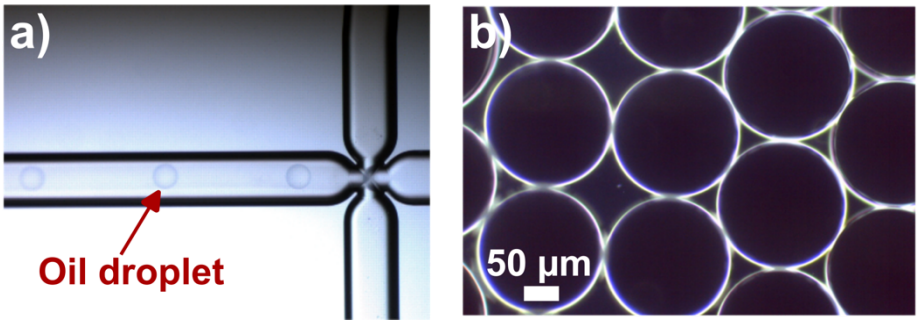

Figure 5. a) Silicone oil emulsion droplets generated in the microfluidic channel (droplets 180 µm in diameter). b) Dark field microscopy of silicone oil emulsion droplets formed with JP at pH 7.4.

Application to increase stain-resistance of a paint system

While gentle encapsulation methods remain a key target for future works, capsules formed using mechanical stirring, heating, and additives can still be added to paint to explore the beneficial properties that JP-encapsulated oils can confer onto coatings. Encapsulated silicone oil has been shown to improve the long-term hydrophobicity of paint film,[9] however, free silicone oils in paint can cause cratering due to local dewetting effects due to the low surface tension of free silicone oil in system.[59, 60] The 5 µm diameter silicone oil droplets encapsulated by Stable JP were added to a paint system, and their impact on stain resistance performance assessed. The addition of the capsules demonstrated a superior stain resistance (Figure 6c) relative the plain commercial paint (Figure 6e), with all the stains other than coffee. However, the capsules also showed evidence of cratering in the paint (Fig 6a), indicating dewetting caused by free silicone oil in the system due to leakage from incomplete encapsulation, and to capsule breakage during integration.

To reduce the cratering effect resulting from the non-encapsulated silicone oil, silica nanoparticles were added to the dispersion of silicone oil capsules for 24 hours and then the dispersion was added to a commercial paint formula. Silicone oil spontaneously forms covalent bonds with silicon oxide surface groups on silica and other oxides, forming hydrophobized silica (Fig. S4).[61-63] The effect was a mild reduction in the cratering effect due to the removal of the free silicone oil (Figure 6b) while maintaining the stain resistance (Figure 6d).

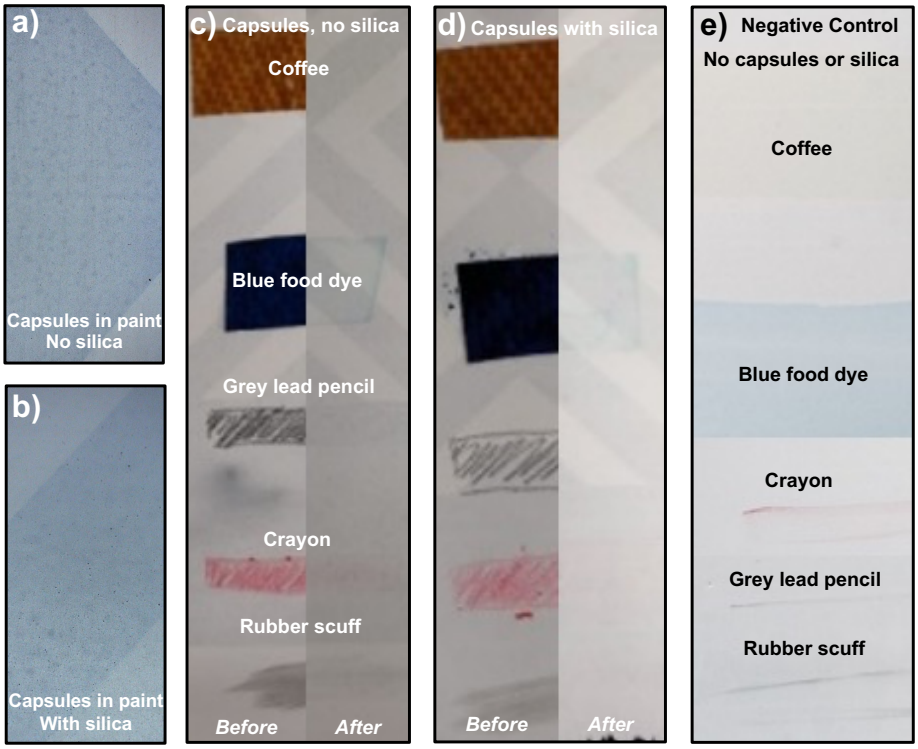

Figure 6. a) A commercial paint film containing JP-encapsulated silicone oil emulsions shows cratering effect due to unencapsulated silicone oil. b) Incubating JP-encapsulated silicone oil emulsions with silica nanoparticles before integration into commercial paint shows reduced cratering. c-d) Paint with capsules shows improved stain resistance, with or without silica nanoparticles respectively, relative to the control of e) stain resistance on the commercial paint without capsules or silica nanoparticles.

These findings show that the current methodology using JP suspensions incompletely encapsulate silicone oil, but the capsules confer benefits to paint coatings, especially when combined with a silica particle treatment to remove cratering. Further tuning of Janus balance *via* modification of the chemistry and proportions of Janus lobes[28] as well as expanding these explorations to other viable oil systems should allow for manipulation of the interfacial adsorption kinetics and thermodynamics, to allow for a greater control of JP adsorption and encapsulation.[55] Further exploration of polymer T_g should also allow for manipulation of film formation, and capsule thickness, which can further influence release kinetics and payload retention to reduce leakage.[64 65]

Conclusions

Improvements were made to previously synthesized film-forming snowman Janus Particles by introducing sulfonate groups and steric stabilizing groups to make them more stable. When adsorbed at oil/water or air/water interfaces, film-forming polymeric Janus nanoparticles were shown to self-assemble and coalesce, forming a polymer nanothin shell (25-250 nm thick) that can be used to encapsulate silicone oil droplets, the first example of these systems encapsulating liquids. The topography of the films deposited from the air/water interface onto solid substrates suggests that the particles can partially orient at the air–water interface. Different encapsulation approaches were tested and the addition of viscosity modifiers and surfactants to the mechanical vortexing process was found to be most effective: capsules could be formed with high viscosity silicone oil, with significantly reduced diameter, from 100 - 500 μm down to 5 μm. Without flocculation, additives, or heating, microfluidics could produce monodisperse encapsulated droplets of 180 μm, showing potential for future novel applications in encapsulating sensitive active agents in latex-compatible systems, although they were too fragile to integrate into paint. When mechanically formed JP-capsules containing silicone oil were integrated into a commercial paint formulation, they improved stain resistance but caused cratering, indicating that silicone oil encapsulation was incomplete. The cratering could be mitigated by incubating the capsules with silica nanoparticles, binding excess silicone oil, while preserving the improvements in stain resistance. Besides the paint sector, the ability to encapsulate oils without the need of polymerisation could benefit many industries in which labile ingredients are used, such as agrochemicals, cosmetics, and pharmaceuticals. Future studies will clarify more quantitatively rheological properties of the interfacial layers, as well as the kinetics of encapsulation and of release of the silicone oil, but the current study should direct studies into the use of film forming Janus nanoparticles for polymerisation- and cross-linking free encapsulation approaches.

Supporting Information

- Additional zeta potential, DLS, contact angle, GPC characterization and microfluidic encapsulation screening data, AFM, TEM and optical micrographs

Acknowledgements

The authors acknowledge funding from the Australian Research Council Linkage Scheme (LP200200806 and LP170100090). The authors acknowledge the technical and scientific assistance of Sydney Microscopy & Microanalysis, the University of Sydney node of Microscopy Australia, Dr Liwen Zhu for preliminary studies underpinning this work, Dr Minh Lam for TEM/SEM imaging, and Dr Vien Huynh for GPC analysis.

Author contributions:

Geosmin Turpin (pendant drop experimental design, JP characterisation, manuscript design, writing, editing), Duc Nguyen (JP synthesis and characterisation, capsule optimisation), Kathryn Sypkes (pendant drop tensiometry experiments), Christopher Vega-Sánchez (microfluidic design and experiments), Tim Davey (advice on JP synthesis and use), Brian Hawkett (experimental design, procurement of funding), Chiara Neto (experimental design, manuscript editing, procurement of funding).

References

(1) Vlachopoulos, A.; Karlioti, G.; Balla, E.; Daniilidis, V.; Kalamas, T.; Stefanidou, M.; Bikiaris, N. D.; Christodoulou, E.; Koumentakou, I.; Karavas, E. Poly (lactic acid)-based microparticles for drug delivery applications: An overview of recent advances. *Pharmaceutics* **2022**, *14* (2), 359.
(2) Yan, C.; Kim, S. R. Microencapsulation for Pharmaceutical Applications: A Review. *ACS Appl Bio Mater* **2024**, *7* (2), 692-710.
(3) Casanova, F.; Santos, L. Encapsulation of cosmetic active ingredients for topical application–a review. *J. Microencapsul.* **2016**, *33* (1), 1-17.
(4) Dhakal, S. P.; He, J. Microencapsulation of vitamins in food applications to prevent losses in processing and storage: A review. *Food Res. Int.* **2020**, *137*, 109326.
(5) Calderón-Oliver, M.; Ponce-Alquicira, E. The role of microencapsulation in food application. *Molecules* **2022**, *27* (5), 1499.
(6) Sadabadi, H.; Allahkaram, S. R.; Kordijazi, A.; Rohatgi, P. K. Self-healing coatings loaded by nano/microcapsules: A review. *Prot. Met. Phys. Chem. Surf.* **2022**, *58* (2), 287-307.
(7) Li, Y.; Wang, G.; Guo, Z.; Wang, P.; Wang, A. Preparation of microcapsules coating and the study of their bionic anti-fouling performance. *Materials* **2020**, *13* (7), 1669.
(8) Park, D. H.; Nguyen, X. D.; Jeon, H. J.; Go, J. S. Recoverable self-cleaning surface formed by nanostructured microcapsules encapsulating hydrophobic agent. *J. Micromech. Microeng.* **2021**, *31* (4), 045002.
(9) Pang, H.; Zhou, S.; Gu, G.; Wu, L. Long-term hydrophobicity and ice adhesion strength of latex paints containing silicone oil microcapsules. *J. Adhes. Sci. Technol.* **2013**, *27* (1), 46-57.
(10) Bhatt, B.; Gupta, S.; Sharma, M.; Khare, K. Dewetting of non-polar thin lubricating films underneath polar liquid drops on slippery surfaces. *J. Colloid Interface Sci.* **2022**, *607*, 530-537.

(11) Bah, M. G.; Bilal, H. M.; Wang, J. Fabrication and application of complex microcapsules: A review. *Soft Matter* **2020**, *16* (3), 570-590.
(12) Chu, L.-Y.; Utada, A. S.; Shah, R. K.; Kim, J.-W.; Weitz, D. A. Controllable monodisperse multiple emulsions. *Angew. Chem. - Int. Ed.* **2007**, *46* (47), 8970.
(13) Wang, W.; Zhang, M.-J.; Chu, L.-Y. Functional polymeric microparticles engineered from controllable microfluidic emulsions. *Acc. Chem. Res.* **2014**, *47* (2), 373-384.
(14) Goodarzi, F.; Zendehboudi, S. A comprehensive review on emulsions and emulsion stability in chemical and energy industries. *Can. J. Chem. Eng.* **2019**, *97* (1), 281-309.
(15) Kosarli, M.; Bekas, D. G.; Tsirka, K.; Baltzis, D.; Vaimakis-Tsogkas, D. T.; Orfanidis, S.; Papavassiliou, G.; Paipetis, A. S. Microcapsule-based self-healing materials: Healing efficiency and toughness reduction vs. capsule size. *Compos. B: Eng.* **2019**, *171*, 78-86.
(16) Rodriguez, A. M. B.; Binks, B. P. Capsules from Pickering emulsion templates. *Curr. Opin. Colloid Interface Sci.* **2019**, *44*, 107-129.
(17) Kientz, E.; Holl, Y. Distribution of surfactants in latex films. *Colloids Surf. A: Physicochem. Eng. Asp.* **1993**, *78*, 255-270.
(18) Butler, L. N.; Fellows, C. M.; Gilbert, R. G. Effect of surfactant systems on the water sensitivity of latex films. *J. Appl. Polym. Sci.* **2004**, *92* (3), 1813-1823.
(19) Hagan, E. W.; Charalambides, M. N.; Young, C. R.; Learner, T. J.; Hackney, S. Viscoelastic properties of latex paint films in tension: Influence of the inorganic phase and surfactants. *Prog. Org. Coat.* **2010**, *69* (1), 73-81.
(20) Honciuc, A. Amphiphilic Janus particles at interfaces. *Flowing Matter* **2019**, 95-136.
(21) Correia, E. L.; Brown, N.; Razavi, S. Janus particles at fluid interfaces: Stability and interfacial rheology. *Nanomaterials* **2021**, *11* (2), 374.
(22) Jiang, Y.; Löbling, T. I.; Huang, C.; Sun, Z.; Müller, A. H.; Russell, T. P. Interfacial assembly and jamming behavior of polymeric Janus particles at liquid interfaces. *ACS Appl. Mater. Interfaces.* **2017**, *9* (38), 33327-33332.
(23) Ruhland, T. M.; Gröschel, A. H.; Ballard, N.; Skelhon, T. S.; Walther, A.; Müller, A. H.; Bon, S. A. Influence of Janus particle shape on their interfacial behavior at liquid–liquid interfaces. *Langmuir* **2013**, *29* (5), 1388-1394.
(24) Wu, D.; Binks, B. P.; Honciuc, A. Modeling the interfacial energy of surfactant-free amphiphilic Janus nanoparticles from phase inversion in Pickering emulsions. *Langmuir* **2018**, *34* (3), 1225-1233.
(25) Zhou, Y.; Shen, F.; Zhang, S.; Zhao, Q.; Xu, Z.; Chen, H. Synthesis of Methyl-Capped TiO2–SiO2 Janus Pickering Emulsifiers for Selective Photodegradation of Water-Soluble Dyes. *ACS Appl. Mater. Interfaces.* **2020**, *12* (26), 29876-29882.
(26) Passas-Lagos, E.; Schuth, F. Amphiphilic pickering emulsifiers based on mushroom-type Janus particles. *Langmuir* **2015**, *31* (28), 7749-7757.
(27) Duong, H.; Nguyen, D.; Neto, C.; Hawkett, B. Synthesis and applications of polymeric Janus nanoparticles. In *Soft, Hard, and Hybrid Janus Structures: Synthesis, Self-Assembly, and Applications*, World Scientific, 2018.
(28) Jiang, S.; Granick, S. Janus balance of amphiphilic colloidal particles. *J. Chem. Phys.* **2007**, *127* (16), 161102.
(29) Binks, B.; Fletcher, P. Particles adsorbed at the oil− water interface: A theoretical comparison between spheres of uniform wettability and “Janus” particles. *Langmuir* **2001**, *17* (16), 4708-4710.
(30) Aveyard, R. Can Janus particles give thermodynamically stable Pickering emulsions? *Soft Matter* **2012**, *8* (19), 5233-5240.
(31) Xie, S.; Chen, S.; Zhu, Q.; Li, X.; Wang, D.; Shen, S.; Jin, M.; Zhou, G.; Zhu, Y.; Shui, L. Janus nanoparticles with tunable amphiphilicity for stabilizing pickering-emulsion droplets

via assembly behavior at oil–water interfaces. *ACS Appl. Mater. Interfaces.* **2020**, *12* (23), 26374-26383.
(32) van Rijn, P.; Mougin, N. C.; Franke, D.; Park, H.; Böker, A. Pickering emulsion templated soft capsules by self-assembling cross-linkable ferritin–polymer conjugates. *Chem. Commun.* **2011**, *47* (29), 8376-8378.
(33) Zheng, T.; Pilla, S. Encapsulation of hydrophilic payload by PU-PMF capsule: Effect of melamine-formaldehyde pre-polymer content, pH and temperature on capsule morphology. *Colloids Surf. A: Physicochem. Eng. Asp.* **2018**, *542*, 59-67.
(34) Yang, Y.; Ning, Y.; Wang, C.; Tong, Z. Capsule clusters fabricated by polymerization based on capsule-in-water-in-oil Pickering emulsions. *Polym. Chem.* **2013**, *4* (21), 5407-5415.
(35) Liu, L.; Wei, J.; Ho, K. M.; Chiu, K. Y.; Ngai, T. Capsules templated from water-in-oil Pickering emulsions for enzyme encapsulation. *J. Colloid Interface Sci.* **2023**, *629*, 559-568.
(36) Nallamilli, T.; Binks, B. P.; Mani, E.; Basavaraj, M. G. Stabilization of Pickering emulsions with oppositely charged latex particles: influence of various parameters and particle arrangement around droplets. *Langmuir* **2015**, *31* (41), 11200-11208.
(37) Liu, Z.; Hu, M.; Zhang, S.; Jiang, L.; Xie, F.; Li, Y. Oil-in-water Pickering emulsion stabilization with oppositely charged polysaccharide particles: chitin nanocrystals/fucoidan complexes. *J. Sci. Food Agric.* **2021**, *101* (7), 3003-3012.
(38) Wei, D.; Ge, L.; Lu, S.; Li, J.; Guo, R. Janus particles templated by Janus emulsions and application as a pickering emulsifier. *Langmuir* **2017**, *33* (23), 5819-5828.
(39) Pham, B. T. T.; Such, C. H.; Hawkett, B. S. Synthesis of polymeric janus nanoparticles and their application in surfactant-free emulsion polymerizations. *Polym. Chem.* **2015**, *6* (3), 426-435, 10.1039/C4PY01125B.
(40) Nguyen, D.; Huynh, V. T.; Serelis, A. K.; Davey, T.; Paravagna, O.; Such, C. H.; Hawkett, B. S. Janus particles by simplified RAFT-based emulsion polymerization process for polymer coating. *Colloid. Polym. Sci.* **2022**, *300* (4), 341-349.
(41) Nguyen, D.; Zhu, L.; Huynh, V. T.; Azniwati, A.-A.; Pham, N. T. H.; Lam, M. T.; Serelis, A. K.; Davey, T.; Such, C.; Neto, C.; Hawkett, B. S. Soft–hard Janus nanoparticles for polymer encapsulation of solid particulate. *Polym. Chem.* **2020**, *11* (35), 5610-5618.
(42) Nguyen, T.; Grosberg, A. Y.; Shklovskii, B. Screening of a charged particle by multivalent counterions in salty water: Strong charge inversion. *J. Chem. Phys.* **2000**, *113* (3), 1110-1125.
(43) Wang, X.; Lee, S. Y.; Miller, K.; Welbourn, R.; Stocker, I.; Clarke, S.; Casford, M.; Gutfreund, P.; Skoda, M. W. Cation bridging studied by specular neutron reflection. *Langmuir* **2013**, *29* (18), 5520-5527.
(44) Oncsik, T.; Trefalt, G.; Csendes, Z.; Szilagyi, I.; Borkovec, M. Aggregation of negatively charged colloidal particles in the presence of multivalent cations. *Langmuir* **2014**, *30* (3), 733-741.
(45) Ibarra-Montaño, E. L.; Rodríguez-Laguna, N.; Sánchez-Hernández, A.; Rojas-Hernández, A. Determination of pKa values for acrylic, methacrylic and itaconic acids by 1H and 13C NMR in deuterated water. *J. Appl. Sol. Chem. Model.* **2015**, *4* (1), 7.
(46) Riechers, B.; Maes, F.; Akoury, E.; Semin, B.; Gruner, P.; Baret, J.-C. Surfactant adsorption kinetics in microfluidics. *PNAS* **2016**, *113* (41), 11465-11470.
(47) Marinova, K.; Alargova, R.; Denkov, N.; Velev, O.; Petsev, D.; Ivanov, I.; Borwankar, R. Charging of oil− water interfaces due to spontaneous adsorption of hydroxyl ions. *Langmuir* **1996**, *12* (8), 2045-2051.
(48) Hoberg, A.-M.; Haddleton, D. M.; Derrick, P. J.; Jackson, A. T.; Scrivens, J. H. The effect of counter ions in matrix-assisted laser desorption/ionization of poly (methyl methacrylate). *Eur. Mass Spectrom.* **1998**, *4* (6), 435-440.

(49) Moncho-Jordá, A.; Martınez-López, F.; Hidalgo-Alvarez, R. The effect of the salt concentration and counterion valence on the aggregation of latex particles at the air/water interface. *J. Colloid Interface Sci.* **2002**, *249* (2), 405-411.
(50) Luu, X.-C.; Striolo, A. Ellipsoidal Janus nanoparticles assembled at spherical oil/water interfaces. *J. Phys. Chem. B* **2014**, *118* (47), 13737-13743.
(51) Knapp, E. M.; Dagastine, R. R.; Tu, R. S.; Kretzschmar, I. Effect of Orientation and Wetting Properties on the Behavior of Janus Particles at the Air–Water Interface. *ACS Appl. Mater. Interfaces.* **2019**, *12* (4), 5128-5135.
(52) Park, B. J.; Brugarolas, T.; Lee, D. Janus particles at an oil–water interface. *Soft Matter* **2011**, *7* (14), 6413-6417.
(53) Hidalgo, R.; Lopez-Diaz, D.; Velázquez, M. M. Graphene oxide thin films: influence of chemical structure and deposition methodology. *Langmuir* **2015**, *31* (9), 2697-2705.
(54) Vogel, N.; Retsch, M.; Fustin, C.-A.; Del Campo, A.; Jonas, U. Advances in colloidal assembly: the design of structure and hierarchy in two and three dimensions. *Chem. Rev.* **2015**, *115* (13), 6265-6311.
(55) Banik, M.; Sett, S.; Bakli, C.; Raychaudhuri, A. K.; Chakraborty, S.; Mukherjee, R. Substrate wettability guided oriented self assembly of Janus particles. *Scientific Reports* **2021**, *11* (1), 1182.
(56) Keddie, J. L. Film formation of latex. *Materials Science and Engineering: R: Reports* **1997**, *21* (3), 101-170.
(57) Routh, A. F.; Russel, W. B. Deformation Mechanisms during Latex Film Formation: Experimental Evidence. *Industrial & Engineering Chemistry Research* **2001**, *40* (20), 4302-4308.
(58) Boxall, J. A.; Koh, C. A.; Sloan, E. D.; Sum, A. K.; Wu, D. T. Droplet size scaling of water-in-oil emulsions under turbulent flow. *Langmuir* **2012**, *28* (1), 104-110.
(59) Flitton, J.; King, J. Surface-tension-driven dewetting of Newtonian and power-law fluids. *J. Eng. Math.* **2004**, *50*, 241-266.
(60) Bubat, A.; Scholz, W. Silicone additives for paints and coatings. *Chimia* **2002**, *56* (5), 203-203.
(61) Krumpfer, J. W.; McCarthy, T. J. Rediscovering silicones:“unreactive” silicones react with inorganic surfaces. *Langmuir* **2011**, *27* (18), 11514-11519.
(62) Teisala, H.; Baumli, P.; Weber, S. A.; Vollmer, D.; Butt, H.-J. r. Grafting silicone at room temperature—a transparent, scratch-resistant nonstick molecular coating. *Langmuir* **2020**, *36* (16), 4416-4431.
(63) Gresham, I. J.; Neto, C. Advances and challenges in slippery covalently-attached liquid surfaces. *Adv. Colloid Interface Sci.* **2023**, 102906.
(64) Wang, A.; Edwards, B. J. Modeling controlled release from hollow porous nanospheres. *Int. J. Heat Mass Transf.* **2016**, *103*, 997-1007.
(65) Vilanova, N.; Rodríguez-Abreu, C.; Fernández-Nieves, A.; Solans, C. Fabrication of novel silicone capsules with tunable mechanical properties by microfluidic techniques. *ACS Appl. Mater. Interfaces.* **2013**, *5* (11), 5247-5252.

ToC Image: